OPEN ACCESS
Global Journal of Research in Engineering & Computer Sciences
ISSN: 2583-2727 (Online)
Volume 04| Issue 06 | Nov.-Dec. | 2024
Journal homepage: https://gjrpublication.com/gjrecs/
Review Article

Feedback Linearization Based Model Predictive control of Rotor Speed of DFIG-WT

Abdussamad Maaruf Fagge[1], Abubakar Surajo Imam[2], Nurudeen Danladi Garba[3], Muhammad Muneer Haruna[4], *Muhammad Ahmad Baballe[5]

[1]National Space Research and Development Agency, Abuja, Nigeria.
[2, 3, 4, 5]Department of Mechatronics Engineering, Nigerian Defence Academy (NDA), Kaduna, Nigeria.
DOI: 10.5281/zenodo.14488485 **Submission Date:** 10 Nov. 2024 | **Published Date:** 15 Dec. 2024

***Corresponding author:** Muhammad Ahmad Baballe
Department of Mechatronics Engineering, Nigerian Defence Academy (NDA), Kaduna, Nigeria.
ORCID: 0000-0001-9441-7023

Abstract
In this work, full order nonlinear model of Wind Turbine Doubly-Fed Induction Generator (DFIG-WT), including stator dynamics has been considered. Nonlinear Multi-Input-Multi-Mutput (MIMO) feedback linearization controller has been designed to control the rotor speed of Doubly-Fed Induction Generator (DFIG) in Wind Energy Conversion System (WECS). The desired states are chosen to drive the system at optimum rotor speed for maximum power point tracking. Due to unpredictable nature of wind speed, the rotor may fail to retain the optimal speed. Model Predictive Controller (MPC) with output constrain has been designed for the rotor side converter to ensure that the rotor retain the optimal speed for all operating points. It also improves the transient state of the rotor speed.

Keywords: *DFIG-WT, Maximum Power Point Tracking, Feedback linearization, Model predictive control.*

I. INTRODUCTION

Power generation from renewable energy is ever growing due to global warming disquiets, hikes in oil prices and government policies towards clean energy [1-3]. The fastest growing source of renewable energy is wind power. The power is generated when the wind speed is enough to rotate the blades of the turbine. The mechanical energy of the rotating blades is converted to electricity by a generator. The preferred location of wind farm is offshore sites where the wind is stronger. Offshore wind farms generate sustainable energy in large quantity contrary to land wind farms [4].

At the moment, doubly-fed induction generator (DFIG) is predominantly used for offshore applications. The main advantages of DFIG for this application are: generating power at low wind speed, generating power at constant frequency and voltage even though the rotor speed is varying, maintaining unity power factor, revamped efficiency and cost effectiveness [5-7].

DFIG has both rotor and stator windings. The rotor windings are connected to the grid via back-back converters. The back-back converters are responsible for regulating both the grid and the rotor currents. Rotor current regulation makes it possible to regulate the active and reactive powers fed to the load from the stators and this is independent of the rotor speed [8,9]. The stator windings are directly connected to the grid by means of the tertiary winding of the transformers.

The control of DFIG is more complex than that of traditional induction generator. The operation of DFIG can be drastically affected by the capricious wind speed if there were no control system is incorporated to it. Similarly, incessant connection of loads to electrical system by the consumers of electricity can severely affect DFIG system without any control [11].

Over the years, many researchers have come up with numerous control techniques to make the DFIG system Robust as well as be able to handle any undesired disturbance it may encounter. The most common of such techniques is conventional vector control. It allows separate control of active and reactive power based on the assumptions that the stator flux is constant and the stator resistance is negligible [12,13]. This method suffers a huge setback under grid fault or when the wind speed is varying. As a result, the stator flux is no longer constant. Furthermore, the dynamics of vector control solely depends on the fine-tuned gains of the Proportional-Integral (PI) controller. However, selecting such gains to ensure stability under varying load is arduous [14].

Moreover, PI controller is applied in [15] to control the grid side converter of DFIG. Further improvement upon this, Fuzzy logic-based controller has been designed in [16] to smoothen the output power oscillation from the grid side converter.

Model Predictive Controller (MPC) can conquer the aforementioned limitation of the PI controller and offer excellent solution for current, flux, power and torque control [17]. MPC is easier to design, cost effective and has faster response than PI controller. Nevertheless, coordinate MPC controllers for rotor side converter (RSC) and stator side converter (SSC) hardly have any significant improvement on the performance of DFIG [14].

Linear Quadratic Regulator (LQR) based on optimal control has been implemented in [18] for pitch control of DFIG wind turbine. The performance of the LQR pitch control is more effective in comparison to PI pitch control. [19] employed Genetic Algorithm (GA) to obtain optimal Q and R matrices. The overall performance of this controller is superior to that in [18].

The aforementioned control techniques are based on the approximated linear model of DFIG near a particular operating point. The controllers give satisfactory performances only near this point. As a result, these controllers are not suitable for DFIG in Wind Energy Conversion System (WECS). This is because DFIG is required to operate under variable speed and wide range of operating points due to capricious wind speed. Therefore, nonlinear control techniques must be employed to cope with the nonlinearities in the system and achieve acceptable wind energy conversion.

Nonlinear robust sliding mode control has been successfully applied in [20] to control the grid voltage. However, the chartering effect augments the mechanical wears. The chartering effect can be attenuated by using higher order sliding mode [21]. Second-Oder sliding mode, also known as super-twisting algorithm has been applied in [22] to attain maximum power point tracking (MPPT). Furthermore, adaptive backstepping control capable of eliminating uncertainties in the system has been described in [23]. Backstepping approach for achieving

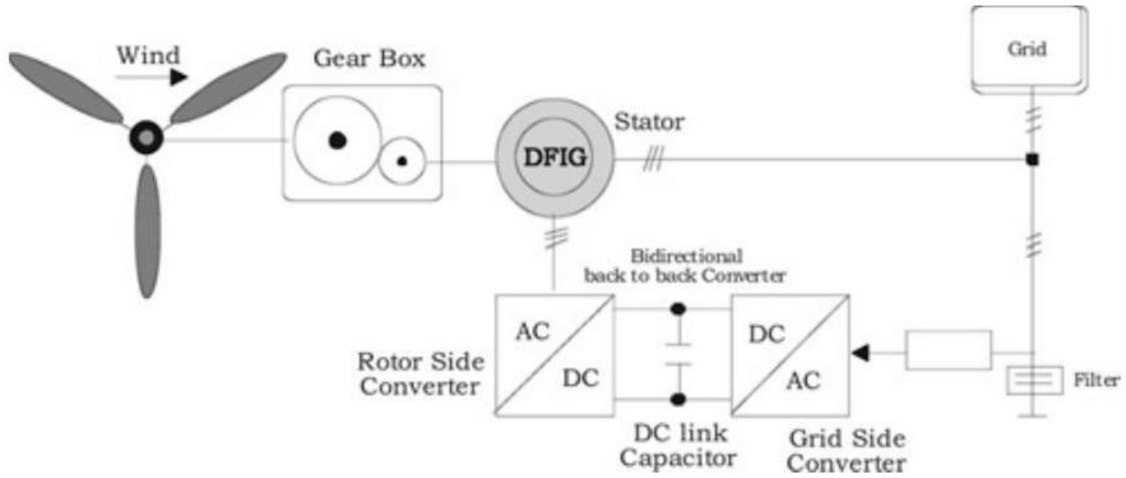

Fig. 1. Wind energy conversion system DFIG [10] reference tracking has been implemented in [23] to control the rotor side converter.

Adaptive feedback linearization together with observer for estimating model uncertainties was employed to improve the performance of wind turbine DFIG [24]. Decentralized feedback linearization controller has been proposed for wind turbine DFIG using differential geometry to improve the transient stability of the power system [25]. feedback linearization control for the current loop was used to attain maximum power point tracking in [26].

The aforementioned nonlinear controllers were based on based reduced order model of DFIG. The stator dynamics was ignored to reduce the order of the model. This greatly reduced the computational complexity and simplifies control design at the expense accuracy.

In this paper, the full order nonlinear model of DFIG together with the stator dynamics has been put into consideration to overcome the limitation of the aforementioned models. Furthermore, four-inputs-four-outputs of the DFIG are considered for control design unlike the aforesaid. Feedback linearization controller has been proposed for input-output decoupling of the system to allow coordinated control of the rotor current and stator flux. This allows the speed to be regulated in such a way to achieve maximum power point tracking. Model Predictive Controller (MPC) with output constraints has been designed for the rotor side to ensure that the rotor retain optimal speed for all operating points. It also improves the transient state of the rotor speed.

The paper is organized as follows; In section I, the mathematical model of DFIG-WT has been derived. In section II, the proposed control schemes have been implemented in section III. The simulation results and the effectiveness of the proposed control schemes have been shown in section IV. The conclusion of the work has been carried out in section V.

II. Mathematical MODELLING OF DFIG

The schematic diagram of the DFIG is depicted in Fig. 1. The full order mathematical model of DFIG-WT in direct and quadrature dq- synchronization frame can be derived as [27, 28]. Application of Kirchhoff's voltage and current laws at all the loops and the nodes of the dq-equivalent circuit diagram [27], the following equations are derived.

$$\frac{d\Psi_{sd}}{dt} = \omega_1 \Psi_{sq} - R_s i_{sd} + u_{sd} \tag{1}$$

$$\frac{d\Psi_{sq}}{dt} = \omega_1 \Psi_{sd} - R_s i_{sq} + u_{sq} \tag{2}$$

$$\frac{d\Psi_{rd}}{dt} = \omega_s \Psi_{rq} - R_r i_{rd} + u_{rd} \tag{3}$$

$$\frac{d\Psi_{rq}}{dt} = \omega_s \Psi_{sd} - R_r i_{rq} + u_{rq} \tag{4}$$

$$\frac{d\omega_r}{dt} = \frac{n_p}{J}(T_e - T_m) \tag{5}$$

$$\Psi_{sd} = L_m i_{rd} + L_s i_{sd} \tag{6}$$

$$\Psi_{sq} = L_m i_{rq} + L_s i_{sq} \tag{7}$$

$$\Psi_{rd} = L_m i_{sd} + L_r i_{rd} \tag{8}$$

$$\Psi_{rq} = L_m i_{sq} + L_r i_{rq} \tag{9}$$

$$T_e = \frac{3L_m n_p}{2L_s}\left(\Psi_{sd} i_{rq} - \Psi_{sq} i_{rd}\right) \tag{10}$$

Where:

u_{sd}, u_{sq}	d-q components of stator voltage
i_{sd}, i_{sq}	d-q components of stator current
Ψ_{sd}, Ψ_{sq}	d-q components of stator flux
u_{rd}, u_{rq}	d-q components of rotor voltage
i_{rd}, i_{rq}	d-q components of rotor current
Ψ_{rd}, Ψ_{rq}	d-q components of rotor flux
R_s, R_r	Rotor and stator resistances respectively
L_m, L_r and L_s	Mutual, rotor and stator inductances respectively
J	Generator rotational inertia
T_e	Electromagnetic torque
n_p	Number of pairs of poles

Further evaluations and transforming the state variables, the dynamic equations can be written in the form

$$\dot{x}_1 = -a_1x_1 + a_2x_2 + a_3x_3 + u_1 \quad (11)$$

$$\dot{x}_2 = -a_2x_1 - a_1x_2 + a_3x_4 + u_2 \quad (12)$$

$$\dot{x}_3 = a_4x_1 - a_5x_2x_5 - a_6x_3 + a_7x_4 - a_5u_1 + a_{10}u_3 \quad (13)$$

$$\dot{x}_4 = a_5x_1x_5 + a_4x_2 - a_7x_3 - a_6x_4 - a_5u_2 + a_{10}u_4 \quad (14)$$

$$\dot{x}_5 = a_8(x_1x_4 - x_2x_3) - a_9 \quad (15)$$

$$y_1 = x_1$$

$$y_2 = x_2$$

$$y_3 = x_4$$

$$y_4 = x_5$$

The nonlinear differential equations can be written in normal form:

$$\begin{cases} \dot{x} = f(x) + g(x)u \\ y = h(x) \end{cases} \quad (16)$$

Where:

$x = [x_1 \quad x_2 \quad x_3 \quad x_4 \quad x_5]^{\top} = [\Psi_{sd} \quad \Psi_{sq} \quad i_{rd} \quad i_{rq} \quad \omega_r]^{\top}$

$u = [u_1 \quad u_2 \quad u_3 \quad u_4]^{\top} = [u_{sd} \quad u_{sq} \quad u_{rd} \quad u_{rq}]^{\top}$

$y = [h_1(x) \quad h_2(x) \quad h_3(x) \quad h_4(x)]^{\top} = [x_1 \quad x_2 \quad x_4 \quad x_5]^{\top}$

$$f(x) = \begin{bmatrix} -a_1x_1 + a_2x_2 + a_3x_3 \\ -a_2x_1 - a_1x_2 + a_3x_4 \\ a_4x_1 - a_5x_2x_5 - a_6x_3 + a_7x_4 \\ a_5x_1x_5 + a_4x_2 - a_7x_3 - a_6x_4 \\ a_8(x_1x_4 - x_2x_3) - a_9 \end{bmatrix}$$

$$g(x) = \begin{bmatrix} 1 & 0 & 0 & 0 \\ 0 & 1 & 0 & 0 \\ -a_5 & 0 & a_{10} & 0 \\ 0 & -a_5 & 0 & a_{10} \\ 0 & 0 & 0 & 0 \end{bmatrix}$$

$a_1 = \frac{R_s}{L_s}$, $a_2 = \omega_1$, $a_3 = \beta R_s$, $a_4 = \frac{\beta R_s}{\alpha L_s}$, $a_5 = \frac{\beta}{\alpha}$, $a_6 = \frac{R_r + \beta^2 R_s}{\alpha}$, $a_7 = \omega_s$, $a_8 = \frac{3L_m n_p^2}{2JL_s}$, $a_9 = \frac{n_p}{J}T_m$, $a_{10} = \frac{1}{\alpha}$, $\alpha = \frac{(L_rL_s - L_m^2)}{L_s}$, $\beta = \frac{L_m}{L_s}$

III. Control Design

In this section, the proposed controller scheme is presented. The objective is to regulate the speed to optimal value by coordinated control of rotor current and stator flux.

A. Maximum power point tracking

The amount of power a wind turbine can capture from the wind is given by [26]:

$$p = \frac{1}{2}\rho\pi R_{wt}^2 C_p(\lambda,\theta)V_{wind}^3 \quad (17)$$

$$\lambda = \frac{\omega_r R_{wt}}{K_1 V_{wind}} \quad (18)$$

The power coefficient is a function of both pitch angle θ and tip speed ratio λ defined by [27]:

$$C_p(\lambda,\theta) = 0.5176\left(\frac{116}{\lambda_j} - 0.4\theta - 5\right)e^{\frac{-21}{\lambda_j}} + 0.0068\lambda \quad (19)$$

$$\frac{1}{\lambda_j} = \frac{1}{\lambda_j + 0.08\theta} - \frac{0.035}{\beta^3 + 1} \quad (20)$$

Where ρ is air density, R_{wt} is radius of wind turbine, V_{wind} is wind speed, $C_p(\lambda,\theta)$ is power coefficient, θ is pitch angle and λ is tip speed ratio.

Wind turbine can generate maximum power provided that the power coefficient $C_p(\lambda,\theta)$ is maximum for any wind speed within the wide operation region of the turbine. The power coefficient $C_p(\lambda,\theta)$ can be maximized by maintaining optimal value of the tip speed ratio λ_{opt} and fixed pitch angle θ.

$$C_{p\max} = C_p\left(\lambda_{opt},\theta\right) \tag{21}$$

Therefore, the desired optimal speed is given by:

$$\omega_{rd} = \frac{K_1\lambda_{opt}}{R_{wt}}V_{wind} \tag{22}$$

B. Feedback linearization

the nonlinear MIMO system is decoupled and linearized based on input-output feedback linearization technique. The output of the system, y_k, is differentiated until the input, u_k, ($k = 1,2,3,4$) appears [26].

$$y_k^{r_k} = L_f^{r_k}h_k + \sum_{k=1}^{n} L_{g_k}L_f^{r_k-1}h_k u_k;\ k = 1,2,3,4 \tag{23}$$

where $y_k^{r_k}$ denotes the $r_k th$-order derivative of y_k. Each y_k has a r_k. The relative degree of the system is the same as the number of states, ($r = 1+1+1+2 = 5 = n$). The third state is an internal state whose stability is proved in the subsequent section. Evaluating the Lie derivatives in (22) leads to the system of equations expressed in the matrices below.

$$\begin{bmatrix}\dot{y}_1\\ \dot{y}_2\\ \dot{y}_3\\ \ddot{y}_4\end{bmatrix} = \begin{bmatrix}L_f h_1(x)\\ L_f h_2(x)\\ L_f h_3(x)\\ L_f^2 h_4(x)\end{bmatrix} + \begin{bmatrix}L_{g1}L_f^0 h_1(x) & L_{g2}L_f^0 h_1(x) & L_{g3}L_f^0 h_1(x) & L_{g4}L_f^0 h_1(x)\\ L_{g1}L_f^0 h_2(x) & L_{g2}L_f^0 h_2(x) & L_{g3}L_f^0 h_2(x) & L_{g4}L_f^0 h_2(x)\\ L_{g1}L_f^0 h_3(x) & L_{g2}L_f^0 h_3(x) & L_{g3}L_f^0 h_3(x) & L_{g4}L_f^0 h_3(x)\\ L_{g1}L_f^1 h_4(x) & L_{g2}L_f^1 h_4(x) & L_{g3}L_f?^1\, h_4(x) & L_{g4}L_f^1 h_4(x)\end{bmatrix}\begin{bmatrix}u_1\\ u_2\\ u_3\\ u_4\end{bmatrix}$$

$$[\dot{y}_1 \quad \dot{y}_2 \quad \dot{y}_3 \quad \ddot{y}_4]^{\top} = A(x) + E(x)u$$

$$A(x) = \begin{bmatrix} -a_1x_1 + a_2x_2 + a_3x_3 \\ -a_2x_1 - a_1x_2 + a_3x_4 \\ a_5x_1x_5 + a_4x_2 - a_7x_3 - a_6x_4 \\ a_8[(-a_1 - a_6)x_1x_4 + (a_2 - a_7)(x_2x_4 + x_1x_3) \\ +(a_1 + a_6)x_2x_3 + a_4x_5(x_1^2 + x_2^2)] \end{bmatrix}$$

$$E(x) = \begin{bmatrix} 1 & 0 & 0 & 0 \\ 0 & 1 & 0 & 0 \\ 0 & -a_5 & 0 & a_{10} \\ q_1 & q_2 & q_3 & q_4 \end{bmatrix}$$

where $q_1 = 2a_8(x_4 + a_5x_2), q_2 = -2a_8(x_3 + a_5x_1), q_3 = -2a_8a_{10}x_2$, and $q_4 = 2a_8a_{10}x_1$, and $\text{Det}(E(x)) = 2a_8x_2a_{10}^2 \neq 0$. Therefore, $E^{-1}(x)$ exists.

The stabilizing inputs for the input-output feedback linearization are defined by; $v = [v_1 \quad v_2 \quad v_3 \quad v_4]$. The linear decoupling between the input and output variables of the system is realized by the control input given below.

$$u = E^{-1}(x)(-A(x) + v) \tag{24}$$

Where:

$$[\dot{y}_1 \quad \dot{y}_2 \quad \dot{y}_3 \quad \ddot{y}_4]^{\top} = [v_1 \quad v_2 \quad v_3 \quad v_4]^{\top}$$

The control objective is to drive the system to point of maximum power required that the defined in the vector, $\eta^d = [\Psi_{sd}^d \quad \Psi_{sq}^d \quad i_{rq}^d \quad w_r^d] = [y_{1d} \quad y_{2d} \quad y_{3d} \quad y_{4d}]$, so that the equilibrium points are shifted to the origin. The error signals are defined as:

$$e = \eta^d - y$$

$$\begin{bmatrix} v_1 \\ v_2 \\ v_3 \\ v_4 \end{bmatrix} = \begin{bmatrix} \dot{y}_{1d} + K_{p1}e_1 + K_{i1}\int \ e_1 dt \\ \dot{y}_{2d} + K_{p2}e_2 + K_{i2}\int \ e_2 dt \\ \dot{y}_{3d} + K_{p3}e_3 + K_{i3}\int \ e_3 dt \\ \ddot{y}_{4d} + K_{p4}e_4 + K_{i4}\int \ e_4 dt \end{bmatrix}$$

$$\begin{cases} \ddot{e}_1 + K_{p1}\dot{e}_1 + K_{i1}e_1 = 0 \\ \ddot{e}_2 + K_{p2}\dot{e}_2 + K_{i2}e_2 = 0 \\ \ddot{e}_3 + K_{p3}\dot{e}_3 + K_{i3}e_3 = 0 \\ \ddot{e}_4 + K_{p4}\dot{e}_4 + K_{i4}e_4 = 0 \end{cases}$$

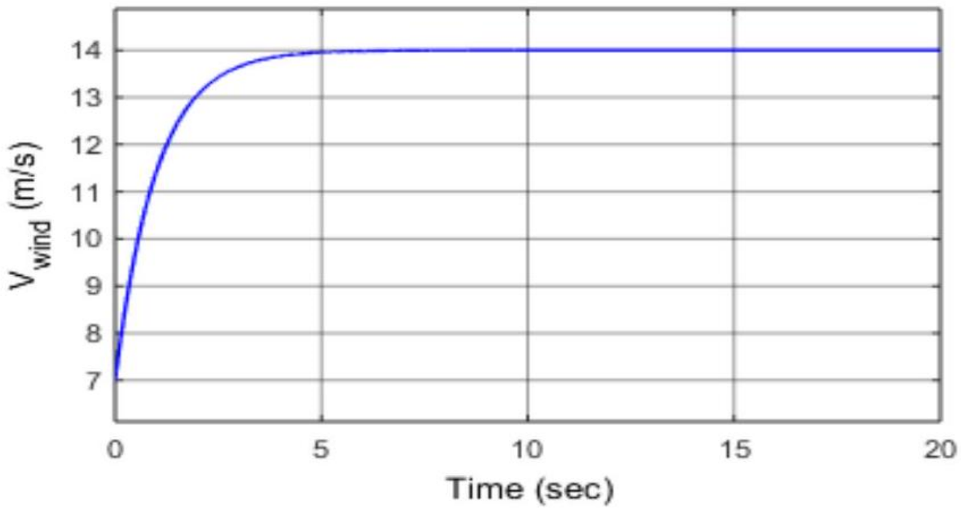

Fig. 2. Wind speed

C. Desired states of the controller

The control targets are the rotor current Ψ and stator flux. The stator oriented-flux frame is aligned with the q-axis. The reference values of the stator flux and its $d - q$ components are given by:

$$\Psi_{sd}^d = 0$$

$$\Psi_{sq}^d = \Psi^d = -\frac{V_s}{\omega_1} = -1$$

$$i_{rq}^d = -\frac{\Psi_s^d}{L_m} = -0.34$$

Where $\omega_1 = 1.0$pu is synchronous speed, $V_s = 1.0$pu is generator rated voltage,

The stabilizing inputs are selected in such a way that the errors converge to zero and the states x_1, x_2, x_4 and x_5 track the reference values $\Psi_{sd}^d, \Psi_{sq}^d, i_{rq}^d$ and w_r^d respectively.

IV. Simulation Result

The performance of the proposed control schemes is evaluated in this section. The parameters of the DFIG-WT are obtained from [32].

The wind speed varies from 7 m/s to 14 m/s and then settles at 14 m/s as shown in Fig. 2. The control objective is to capture maximum power from this wind speed by maximizing the power coefficient and keeping the pitch angle fixed. The maximum power coefficient $(C_{pmax} = 9.0pu)$ is shown in Fig. 3 with the corresponding optimal tip-speed ratio $(\lambda_{\text{opt}} = 0.4569pu)$ at fixed pitch angle $\theta = 1.0$. The turbine will maintain optimal speed and subsequently maximum power as long as the power coefficient remains maximum.

The feedback linearization controller successfully decoupled the rotor and stator dynamics for proper coordinated control. The tuning parameters of the controller are $K_{p1} = 10, K_{i1} = 21, K_{p2} = 4, K_{i2} = 3.5, K_{p3} = 8, K_{i3} = 15, K_{p4} = 22, K_{i4} = 97$.

The d-component and the q-component of the stator flux are shown in Fig. 4 and Fig. 5, respectively. It can be seen that the components of the stator flux have tracked their respective desired values.

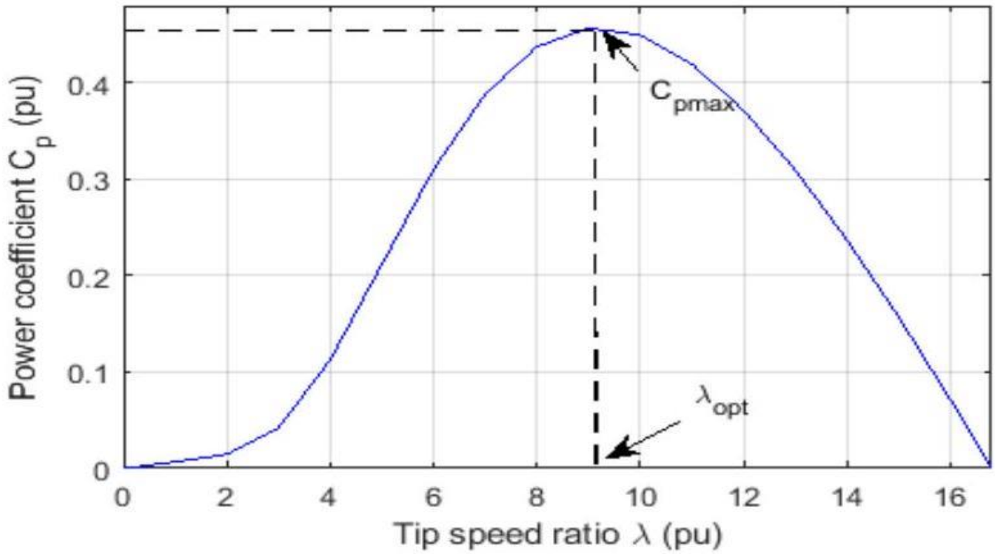

Fig. 3. Power coefficient vs tip-speed ratio

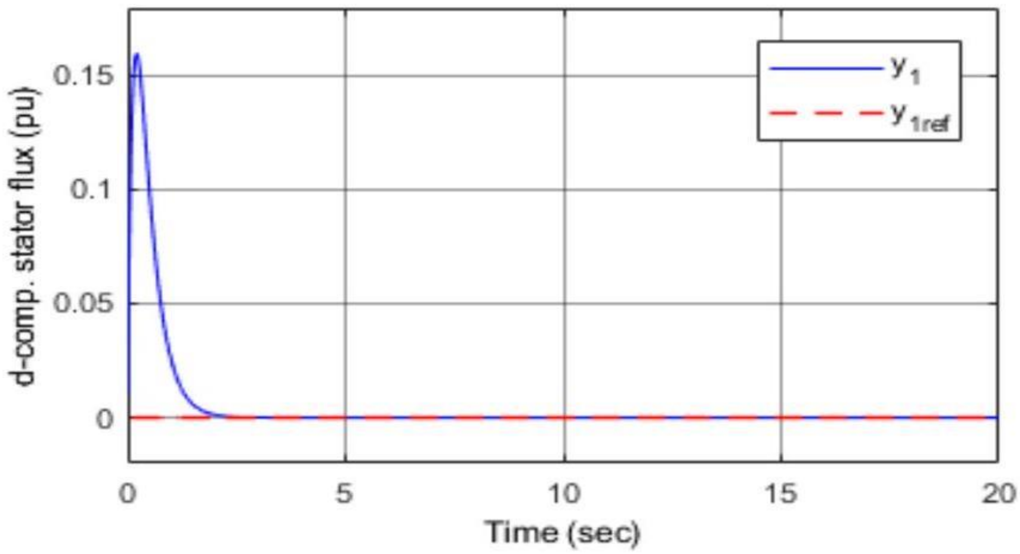

Fig. 4. d-component of stator flux

The q-component of rotor current (y_3) shown in Fig. 6. The speed can be regulated to the optimal speed for the maximum active power generation as shown in Fig. 7.

The tracking errors of the maximum power points converge to zero as shown in Fig. 8.

The control inputs to the DFIG-WT that decouple and ensure the maximum power generation are shown in Fig. 9.

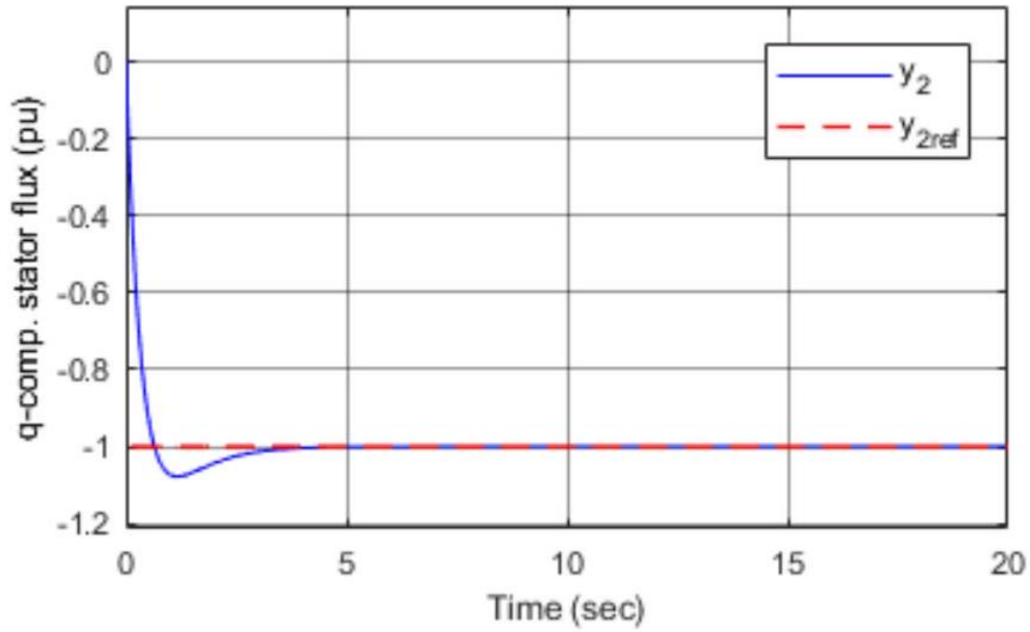

Fig. 5. d-component of stator flux

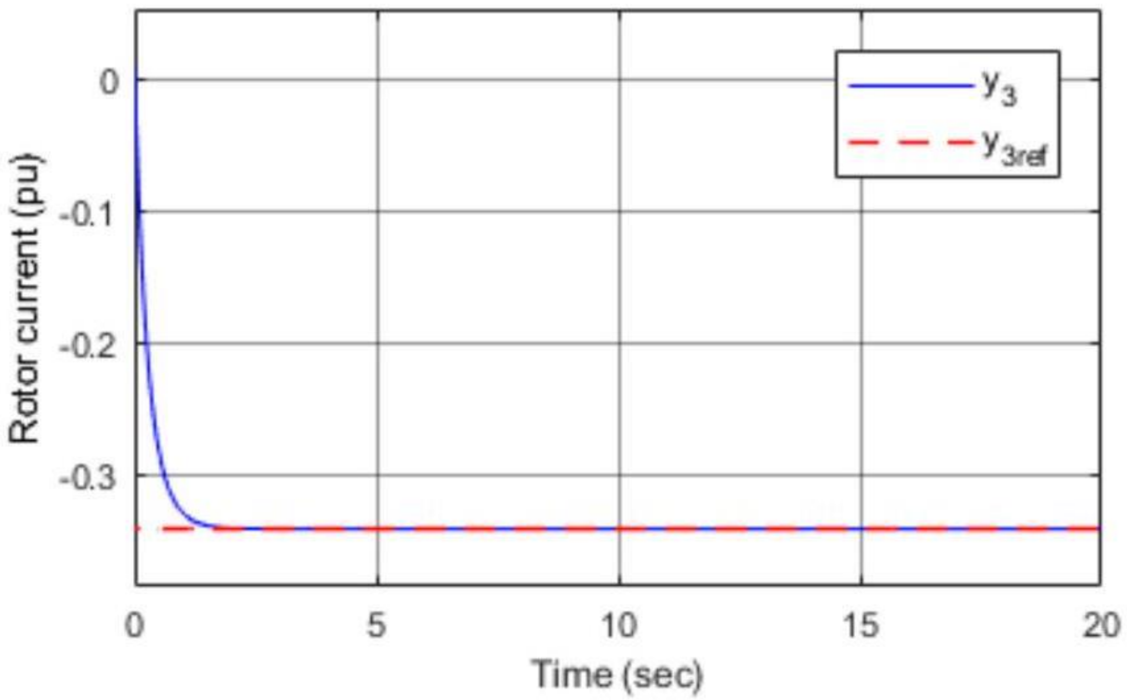

Fig. 6. q-component of rotor current

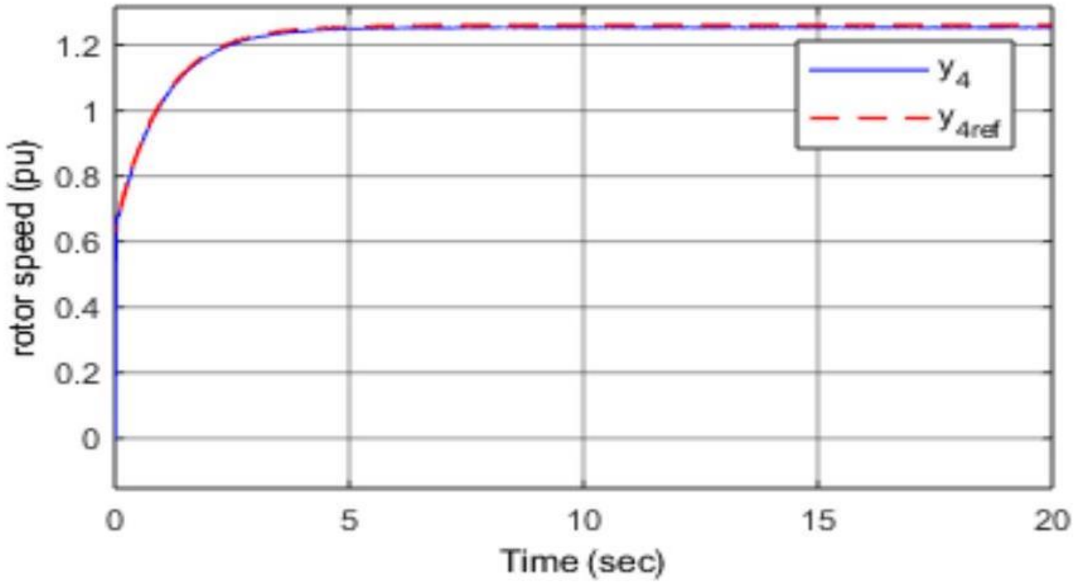

Fig. 7. Optimal rotor speed tracking

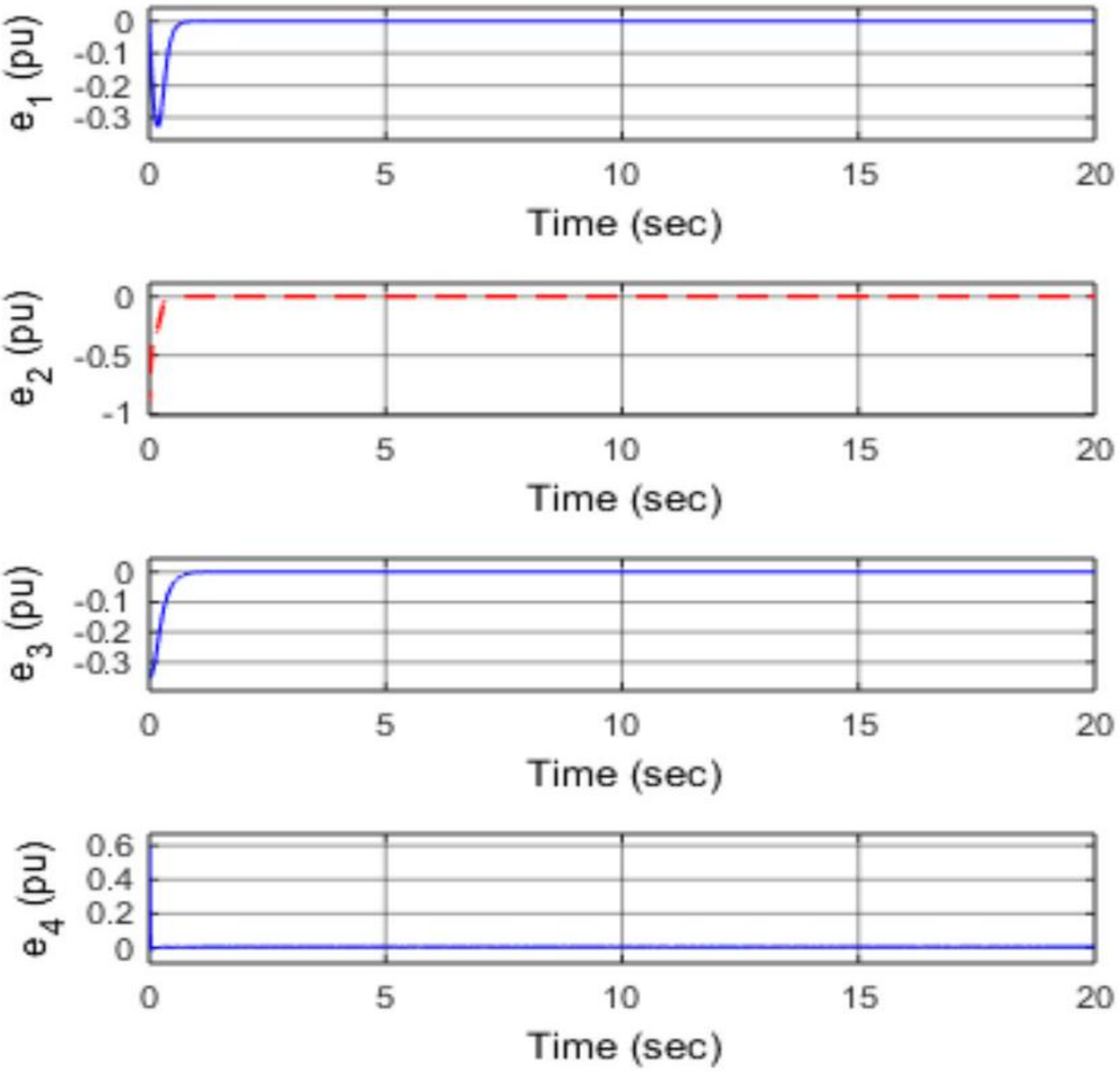

Fig. 8. Tracking errors

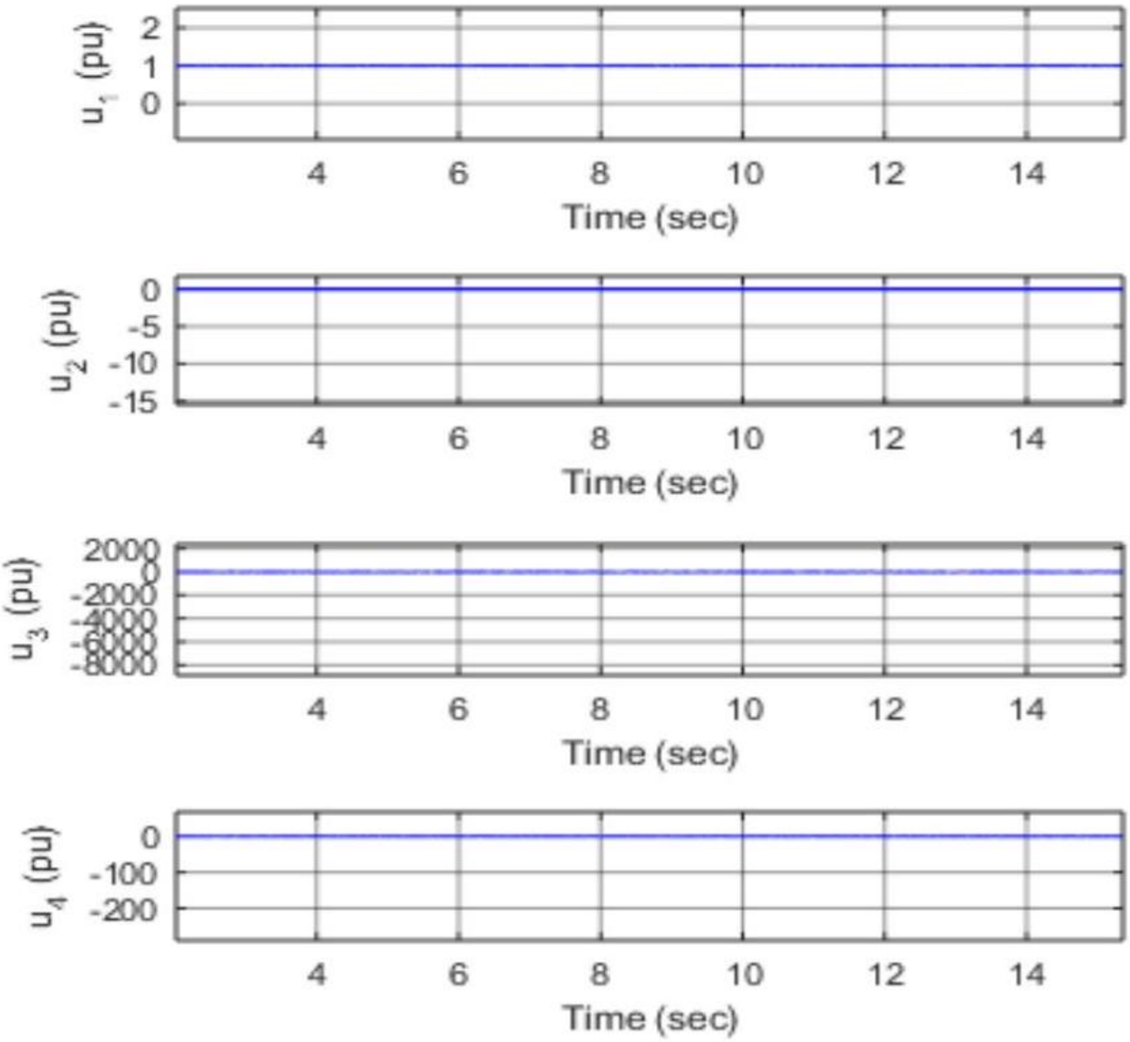

Fig. 9. Control inputs to the DFIG-WT

V. CONCLUSION

Feedback linearization controller has been employed to decoupled and linearized the DFIG-WT system. The coordinated control of rotor current as well as the stator flux has been achieved to regulate the rotor speed to optimal value. At this speed, the wind turbine is able to capture maximum power from the wind. Nevertheless, the rotor speed has some overshoot and it takes time to track the optimal rotor speed for MPPT.

REFERENCES

1. M. Maaruf and M. Khalid. "Global sliding-mode control with fractional order terms for the robust optimal operation of a hybrid renewable microgrid with battery energy storage." Electronics vol. 11, no. 1, pp. 88, 2021.
2. R. Pena, J. C. Clare and G. M. Asher, "Doubly fed induction generator using back-to-back PWM converters and its application to variable speed wind-energy generation," in IEE Proceedings - Electric Power Applications, vol. 143, no. 3, pp. 231-241, May 1996.
3. R. Cardenas, R. Pena, S. Alepuz and G. Asher, "Overview of Control Systems for the Operation of DFIGs in Wind Energy Applications," in IEEE Transactions on Industrial Electronics, vol. 60, no. 7, pp. 27762798, July 2013.
4. M. Maaruf, K.A. Khan and M. Khalid. "Robust control for optimized islanded and grid-connected operation of solar/wind/battery hybrid energy." Sustainability, vol. 14, no. 9, pp. 5673, 2022.
5. M. F. Iacchetti, G. D. Marques and R. Perini, "A Scheme for the Power Control in a DFIG Connected to a DC Bus via a Diode Rectifier," in IEEE Transactions on Power Electronics, vol. 30, no. 3, pp. 1286-1296, March 2015.
6. A review of design consideration for Doubly Fed Induction Generator based wind energy system, Electric Power Systems Research, Volume 160, 2018, Pages 128-141, ISSN 0378-7796,
7. M. Maaruf, Md Shafiullah, A. T. Al-Awami, and F. S. Al-Ismail. "Adaptive nonsingular fast terminal sliding mode control for maximum power point tracking of a wecs-pmsg." Sustainability, vol. 13, no. 23 pp. 13427, 2021

8. Pena, R.; Clare, J.C.; Asher, G.M.: 'A doubly fed induction generator using back-to-back PWM converters supplying an isolated load from a variable speed wind turbine', IEE Proceedings - Electric Power Applications, 1996, 143, (5), p. 380-387
9. R. Cardenas, R. Pena, S. Alepuz and G. Asher, "Overview of Control Systems for the Operation of DFIGs in Wind Energy Applications," in IEEE Transactions on Industrial Electronics, vol. 60, no. 7, pp. 27762798, July 2013.
10. Tazil, M.; Kumar, V.; Bansal, R.C.; Kong, S.; Dong, Z.Y.; Freitas, W.; Mathur, H.D.: 'Three-phase doubly fed induction generators: an overview', IET Electric Power Applications, 2010, 4, (2), p. 75-89.
11. M. Maaruf, S. El Ferik, and M. S. Mahmoud: "Integral sliding mode control with power exponential reaching law for DFIG". In 2020 17th International Multi-Conference on Systems, Signals and Devices (SSD) (pp. 1122-1127). IEEE, 2020.
12. Bo Yang, Lin Jiang, Lei Wang, Wei Yao, Q.H. Wu, Nonlinear maximum power point tracking control and modal analysis of DFIG based wind turbine, International Journal of Electrical Power and Energy Systems, Volume 74, 2016, Pages 429-436, ISSN 0142-0615.
13. G. D. Marques and M. F. Iacchetti, "DFIG Topologies for DC Networks: A Review on Control and Design Features," in IEEE Transactions on Power Electronics, vol. 34, no. 2, pp. 1299-1316, Feb. 2019.
14. S. Yan, A. Zhang, H. Zhang, J. Wang and B. Cai, "An Optimum Design for a DC-Based DFIG System by Regulating Gearbox Ratio," in IEEE Transactions on Energy Conversion, vol. 33, no. 1, pp. 223-231, March 2018.
15. M. Maaruf M, K.A. Khan, M. Khalid, 'Integrated power management and nonlinear-control for hybrid renewable microgrid". In2021 IEEE green technologies conference (GreenTech) 2021 Apr 7 (pp. 176-180). IEEE.
16. Santolo Meo, Alireza Zohoori, Abolfazl Vahedi, Optimal design of permanent magnet flux switching generator for wind applications via artificial neural network and multi-objective particle swarm optimization hybrid approach, Energy Conversion and Management, Volume 110, 2016, Pages 230-239, ISSN 0196-8904.
17. J. Rodriguez et al., "State of the Art of Finite Control Set Model Predictive Control in Power Electronics," in IEEE Transactions on Industrial Informatics, vol. 9, no. 2, pp. 1003-1016, May 2013.
18. K. S. Islam, W. Shen, A. Mahmud, M. A. Chowdhury and J. Zhang, "Stability enhancement of DFIG wind turbine using LQR pitch control over rated wind speed," 2016 IEEE 11th Conference on Industrial Electronics and Applications (ICIEA), Hefei, 2016, pp. 1714-1719.
19. R. Bhushan and K. Chatterjee, Mathematical modeling and control of DFIG-based wind energy system by using optimized linear quadratic regulator weight matrices, International Transaction on Electrical energy system, 27(11), 1-23, 2017.
20. Naggar H. Saad, Ahmed A. Sattar, Abd El-Aziz M. Mansour, Low voltage ride through of doubly-fed induction generator connected to the grid using sliding mode control strategy, Renewable Energy, Volume 80, 2015, Pages 583-594, ISSN 0960-1481.
21. Yaozhen Han, Xiangjie Liu, Continuous higher-order sliding mode control with time-varying gain for a class of uncertain nonlinear systems, ISA Transactions, Volume 62, 2016, Pages 193-201, ISSN 0019-0578.
22. B. Beltran, M. E. H. Benbouzid and T. Ahmed-Ali, "Second-Order Sliding Mode Control of a Doubly Fed Induction Generator Driven Wind Turbine," in IEEE Transactions on Energy Conversion, vol. 27, no. 2, pp. 261-269, June 2012.
23. Patnaik, R.K.; Dash, P.K.: 'Fast adaptive back-stepping terminal sliding mode power control for both the rotor-side as well as grid-side converter of the doubly fed induction generator-based wind farms', IET Renewable Power Generation, 2016, 10, (5), p. 598-610
24. Ghazanfar Shahgholian; Noushaz Izadpanahi. "Improving the performance of wind turbine equipped with DFIG using STATCOM based on input-output feedback linearization controller". Energy Equipment and Systems, 4, 1, 2016, 65-79.
25. F. Wu, X. Zhang, P. Ju and M. J. H. Sterling, "'Decentralized Nonlinear Control of Wind Turbine With Doubly Fed Induction Generator," in IEEE Transactions on Power Systems, vol. 23, no. 2, pp. 613-621, May 2008.
26. X. Lin, K. S. Xiahou, Y. Liu, Y. B. Zhang and Q. H. Wu, 'Maximum power point tracking of DFIG-WT using feedback linearization control based current regulators," 2016 IEEE Innovative Smart Grid Technologies - Asia (ISGT-Asia), Melbourne, VIC, 2016, pp. 718-723.
27. M. Sleiman, B. Kedjar, A. Hamadi, K. Al-Haddad and H. Y. Kanaan, "Modeling, control and simulation of DFIG for maximum power point tracking," 2013 9th Asian Control Conference (ASCC), Istanbul, 2013, pp. 1-6.
28. G. Abad, J. Lopez, M. A. Rodriguez, L. Marroyo, and G. Iwanski, in Doubly Fed Induction Machine: Modeling and Control for Wind Energy Generation, first ed: John Wiley & Sons, Inc., 2011.
29. L. Ljung, System identification: theory for the user. Englewood Cliffs, NJ, USA, 1987.
30. D.Q. Mayne, J.B. Rawlings, C.V. Rao, P.O.M. Scokaert, Constrained model predictive control: Stability and optimality, Automatica, Volume 36, Issue 6, 2000, Pages 789-814, ISSN 0005-1098.
31. Liuping Wang. 2009. Model Predictive Control System Design and Implementation Using MATLAB (1st ed.). Springer Publishing Company, Incorporated.

32. Yuliang Sun, Shaomin Yan, Bin Cai, and Yuqiang Wu, "Maximum Power Point Tracking of DFIG with DC-Based Converter System Using Coordinated Feedback Linearization Control," Mathematical Problems in Engineering, vol. 2018, Article ID 9642123, 12 pages, 2018.

CITATION

Abdussamad M. F., Abubakar S. I., Nurudeen D. G., Muhammad M. H., & Muhammad A. B. (2024). Feedback Linearization Based Model Predictive control of Rotor Speed of DFIG-WT. In Global Journal of Research in Engineering & Computer Sciences (Vol. 4, Number 6, pp. 95–106). https://doi.org/10.5281/zenodo.14488485